A Simulation Study on Sensorless Control of Permanent Magnet Synchronous Motor Drives

Tze-Fun Chan[1], Pieter Borsje[2], Yiu-Kwong Wong[1], and Siu-Lau Ho[1]
[1]Department of EE, The Hong Kong Polytechnic University, Hung Hom, Hong Kong, China
[2]Motion Group Department, ASM Assembly Automation Ltd, Hong Kong, China
eetfchan@polyu.edu.hk, peter.borsje@hccnet.nl, eeykwong@polyu.edu.hk, eeslho@polyu.edu.hk

Abstract-- **This paper presents simple methods for controlling permanent-magnet synchronous motors (PMSM) over a wide speed range without using a shaft position and speed sensor. In classical estimation methods the voltage and current vectors are the input to the estimator, while the rotor position and speed are the output of the estimator. To avoid the drawback of differential and integral operations in conventional sensorless PMSM drives a recursive approach for estimation of the rotor speed and angle is proposed and investigated. The position and speed estimations are based on the back electromotive force (BEMF) method in the $\alpha\beta$-stator reference frame. Two estimation strategies, one using the steady-state equations and the other using the dynamic equations, are compared. Extensive simulation results are given and discussed.**

I. Introduction

Compared with the inverter-fed induction motor drive, the PMSM has no rotor loss and hence it is more efficient and a larger torque-to-weight ratio is achievable. One serious drawback of the classical PMSM, however, is the need for a rotor position sensor, such as a high resolution encoder, for proper control of the inverter switches. The presence of the rotor position sensor (which is a delicate and fragile device) impairs the reliability of the drive system increases the system cost significantly. If the rotor position can be accurately determined without using a sensor, a low-cost, high performance motor drive capable can be produced. In some applications, such a sensorless motor drive system may be the only option, notable examples being electric vehicle and aerospace drive systems.

In recent years, much attention has been paid to sensorless drives [4]. This paper investigates two estimation methods based on the back electromotive force (BEMF).

In classical estimation methods the voltage and current vectors are the input to the estimator, while the rotor position and speed are outputs of the estimator. To avoid the drawback of differential and integral operations in conventional sensorless PMSM drives a recursive approach for estimation of rotor speed and angle will be proposed.

Two estimation algorithms will be considered:

A. Estimation of rotor speed and angle based on the steady-state equations.
B. Estimation of rotor speed and angle based on the dynamic equations.

These methods will be developed and explained in the MATLAB/SIMULINK environment under which the simulation results are obtained.

II. Speed and Current Controller

Fig. 1 shows a schematic diagram of the proposed sensorless PMSM drive.

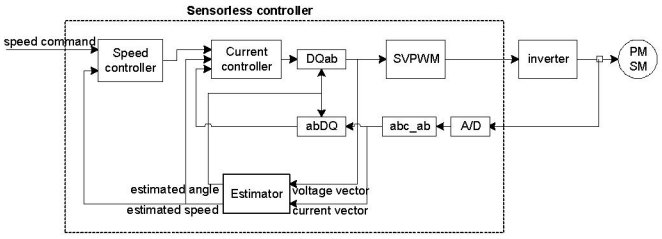

Fig. 1 Schematic diagram of proposed sensorless PMSM drive.

As shown in Fig. 2, a proportional-and-integral (PI) speed controller is implemented to regulate the rotor speed by comparing the reference speed with the estimated speed. The PI controller delivers an output current reference i_q*, while the direct current reference i_d* is set to zero in normal operation to obtain the maximum torque-to-current ratio. At startup and low speeds, i_d* is used to provide bumpless speed change as described in Section IV.

The current controller (Fig. 3) employs two PI blocks to regulate the stator current and employs feed forward control to decouple the dynamics between the applied voltages and the currents. Inputs of the current controller are the current reference and the estimated rotor speed, while its output is the reference voltage. The reference voltage will be applied to a space vector pulse width modulation (SVPWM) unit. The output of the PI controllers are limited.

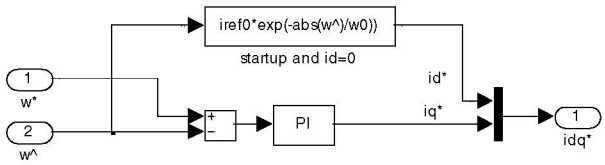

Fig. 2 Speed controller.

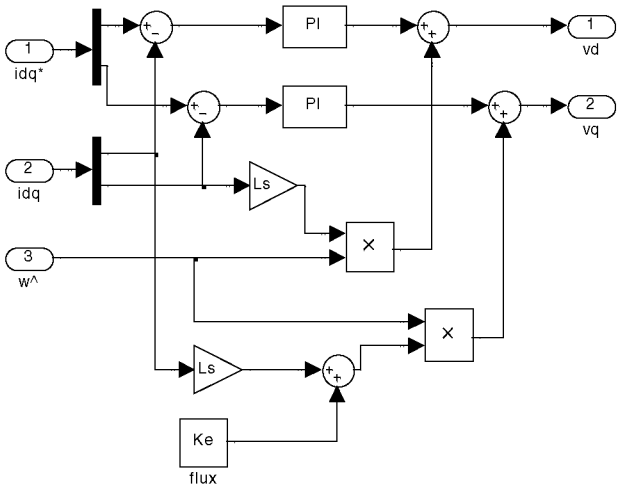

Fig. 3 Current controller.

Instead of using the measured phase voltages, the reference voltages are used as estimator input. This will improve the drive robustness to noise and filtering can be omitted. This approximation is not effective at low speeds because of the dead times and voltage drop of the inverter bridge. This will cause relatively large errors in the voltage estimation. Compensation methods can be used to improve the performance at low speed [5]-[7].

III. PMSM Model

The motor model is described in a stationary two-axis reference frame. The voltages and currents are related to the physical quantities by a simple linear transformation [1], [2].

$$i_\alpha = \frac{2}{3}\left(i_A - \frac{i_B}{2} - \frac{i_C}{2}\right)$$
$$i_\beta = \frac{i_B - i_C}{\sqrt{3}} \quad (1)$$

$$v_\alpha = \frac{2}{3}\left(v_A - \frac{v_B}{2} - \frac{v_C}{2}\right)$$
$$v_\beta = \frac{v_B - v_C}{\sqrt{3}} \quad (2)$$

The dynamic model can be written as

$$L_s \frac{di_\alpha}{dt} = -R_s i_\alpha + \omega\lambda \sin(\theta) + V_\alpha \quad (3)$$

$$L_s \frac{di_\beta}{dt} = -R_s i_\beta - \omega\lambda \cos(\theta) + V_\beta \quad (4)$$

$$T_e = \frac{3}{2} P\lambda\left(i_\beta \cos\theta - i_\alpha \sin\theta\right) \quad (5)$$

$$\frac{J}{P}\frac{d\omega}{dt} = T_e - \frac{B}{P}\omega - T_L \quad (6)$$

$$\frac{d\theta}{dt} = \omega \quad (7)$$

with

$$e_\beta = \omega\lambda\cos(\theta)\,; \quad e_\alpha = \omega\lambda\sin(\theta) \quad (8)$$

IV. Estimation Strategies

A. Steady-state equations

The derivative of the measured current results often in a noisy estimation of position and speed. In steady state drive operation however the current derivative can be well approximated. Let θ be the angle of stator current vector. Then

$$i_\alpha = |i_\alpha|\cos(\theta) \quad (9)$$

$$i_\beta = |i_\beta|\sin(\theta) \quad (10)$$

Supposing stator current magnitude is constant at steady state, derivatives of (9) and (10) are

$$\frac{di_\alpha}{dt} = -|i_\alpha|\sin(\theta)\frac{d\theta}{dt} \quad (11)$$

$$\frac{di_\beta}{dt} = -|i_\beta|\cos(\theta)\frac{d\theta}{dt} \quad (12)$$

At steady state, the current frequency is synchronous with the rotor speed ω_m, i.e.,

$$\frac{d\theta}{dt} = P\omega_m \quad (13)$$

where P is the number of pole-pairs of the PMSM.

Substituting (9) to (12) and (10) to (11) respectively,

$$\frac{di_\alpha}{dt} = -i_\beta P\omega_m \quad (14)$$

$$\frac{di_\beta}{dt} = i_\alpha P\omega_m\,. \quad (15)$$

Substituting (14) to (3) and (15) to (4), respectively,

$$-P\omega_m L_s i_\beta = -R_s i_\alpha + \omega\lambda\sin(\theta) + v_\alpha$$
$$P\omega_m L_s i_\alpha = -R_s i_\beta - \omega\lambda\cos(\theta) + v_\beta \quad (16)$$

or

$$\omega\lambda\sin(\theta) = R_s i_\alpha - P\omega_m L_s i_\beta - v_\alpha \quad (17)$$

$$\omega\lambda\cos(\theta) = -R_s i_\beta - P\omega_m L_s i_\alpha + v_\beta\,. \quad (18)$$

Based on the above equations, the rotor angle may be estimated from stator voltage and current as follows:

$$\tan 2(\hat{\theta}) = \frac{R_s i_\alpha - P\hat{\omega} L_s i_\beta - v_\alpha}{-R_s i_\beta - P\hat{\omega} L_s i_\alpha + v_\beta}, \tag{19}$$

where $\hat{\omega}$ is the estimated rotor mechanical speed.

Eqn. (17) and (18) may be written as

$$\omega\{\lambda \sin(\theta) + L_s i_\beta\} = R_s i_\alpha - v_\alpha \tag{20}$$

$$\omega\{\lambda \cos(\theta) + L_s i_\alpha\} = -R_s i_\beta + v_\beta . \tag{21}$$

From (20) and (21), the rotor speed may be calculated as follows

$$\hat{\omega} = \sqrt{\frac{(R_s i_\alpha - v_\alpha)^2 + (-R_s i_\beta + v_\beta)^2}{\{\lambda \sin(\hat{\theta}) + L_s i_\beta\}^2 + \{\lambda \cos(\hat{\theta}) + L_s i_\alpha\}^2}} . \tag{22}$$

From equations (19) and (22) it can be seen that no derivative of the measured current is used for estimation. This will improve the performance of the drive under noisy operating conditions.

The proposed estimation algorithm is illustrated in Fig. 4.

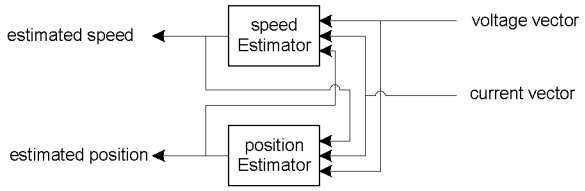

Fig. 4 Dual estimation algorithm with recursive structure.

B. Dynamic equations

In the presented method A the current derivative approximation will not be accurate during ramp up and down of the speed. Large rotor position and speed error estimation will occur. To improve the dynamic performance the dynamic equations from (3)–(8) will be used.

When the rotor speed equals zero, (3) and (4) become

$$L_s \frac{di_\alpha}{dt} = -R_s i_\alpha + v_\alpha \tag{23}$$

$$L_s \frac{di_\beta}{dt} = -R_s i_\beta + v_\beta . \tag{24}$$

Under this condition, the rotor angle can not be estimated from the stator voltages and currents.

Eqns. (3) and (4) may be expressed as

$$\omega\lambda \sin(\theta) = R_s i_\alpha + L_s \frac{di_\alpha}{dt} - v_\alpha \tag{25}$$

$$\omega\lambda \cos(\theta) = -R_s i_\beta - L_s \frac{di_\beta}{dt} + v_\beta . \tag{26}$$

Based on (25) and (26), the rotor angle and speed may be estimated from stator voltage and current as follows:

$$\hat{\theta} = \arctan 2\left(\frac{R_s i_\alpha + L_s \frac{di_\alpha}{dt} - v_\alpha}{-R_s i_\beta - L_s \frac{di_\beta}{dt} + v_\beta} \right) \tag{27}$$

$$\hat{\omega} = \frac{1}{\lambda} \sqrt{(R_s i_\alpha + L_s \frac{di_\alpha}{dt} - v_\alpha)^2 + (-R_s i_\beta - L_s \frac{di_\beta}{dt} + v_\beta)^2} . \tag{28}$$

Notice that the atan2 function [8] is used. This function uses the available phase information in the numerator and denominator to realize a [-π, π] rotor position range.

To avoid noise caused by differential operation, the approximate algorithm shown in Fig. 5 is adopted to implement the current derivatives.

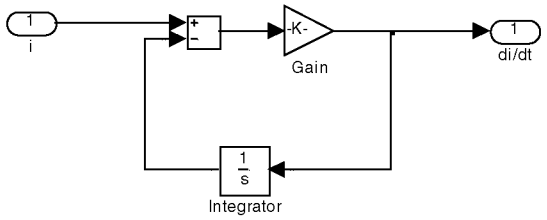

Fig. 5 Approximate derivative.

An inspection of Fig. 5 gives

$$\frac{di}{dt} = \frac{1}{s/K + 1} \cdot si . \tag{29}$$

This approximate algorithm is thus a current derivative with a first order filter.

Both proposed estimation methods A and B have difficulty to work in closed loop. The arctan function in the position estimator is sensitive to noise. Fluctuations in $\hat{\theta}$ directly influence the current control and axis transformations.

To improve the stability and noise performance the back EMF can be estimated using a state filter as shown in Fig. 6. The state filter consists of two parts: the PM model without the back EMF terms (as given in (25) and (26)) and a PI compensator. The back EMF is unmodeled but will be inherently estimated by the PI compensator.

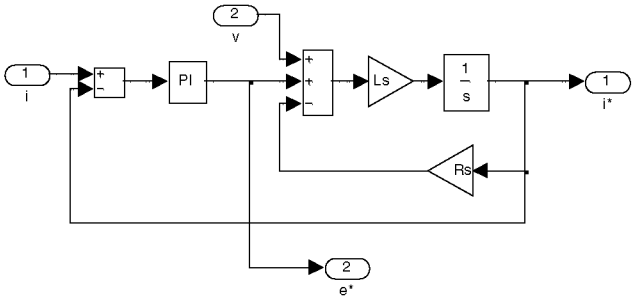

Fig. 6 State filter for estimating back EMF.

Strong PI compensation gives a more accurate estimation and increases the bandwidth, but will also introduce more noise.

The position and speed can now be calculated from

$$\hat{\theta} = \arctan 2\left(\frac{\hat{e}_\alpha}{-\hat{e}_\beta}\right) \tag{30}$$

$$\hat{\omega} = \frac{1}{\lambda}\sqrt{\hat{e}_\alpha{}^2 + \hat{e}_\beta{}^2}\ . \tag{31}$$

The above estimation method is not suitable for speed reversal operation. The sign of the rotor speed needs to be considered in the rotor angle calculation, but this information may be lost due to the division operation of the arctangent function. When the speed is negative, the rotor angle can be described by

$$\frac{\hat{e}_\alpha}{-\hat{e}_\beta} = \frac{\omega\lambda\sin(\hat{\theta})}{\omega\lambda\cos(\hat{\theta})} = \frac{-\sin(\hat{\theta})}{-\cos(\hat{\theta})} = \frac{\sin(\hat{\theta}-\pi)}{\cos(\hat{\theta}-\pi)} = \tan\left(\hat{\theta}-\pi\right) \therefore$$
$$\hat{\theta} = \tan 2^{-1}\left(\frac{\hat{e}_\alpha}{-\hat{e}_\beta}\right) + \pi \tag{32}$$

This problem also appears in many observers in which the currents or their derivatives are used. The estimated position and speed must be corrected for the undetectability between (θ, ω) and (θ + (2k+1)·π, -ω).

The speed direction will be estimated according to Fig. 7.

The phase difference is used to create an adaptive speed estimator which will track the speed signal. The argument arg(exp(j·u)) in Fig. 7 solves the modulus problem. A hysteresis function has been applied to improve the stability during the noisy startup. An adaptive low pass filter is applied to get a smooth speed signal. The bandwidth of the filter is based on (31) and the parameters *K1* and *K2* in Fig. 8. Constant *K1* gives a starting bandwidth for the filter at zero speed. To limit the phase lag of the low pass filter, a bandwidth equal to *K2* times the estimated speed is set by the constant *K2*.

By choosing a constant ratio *K2* for the low pass filter the phase delay can be compensated. Eqn. (33) shows the transfer function of a low pass filter.

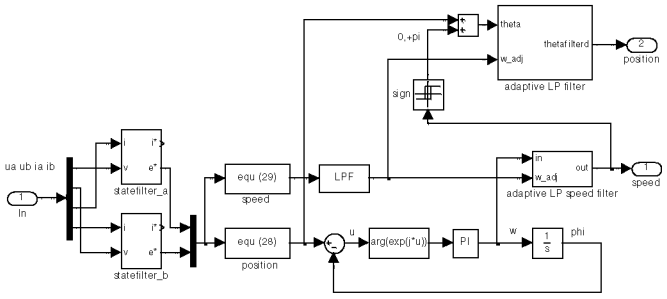

Fig. 7 Estimator with state filter speed and position correction.

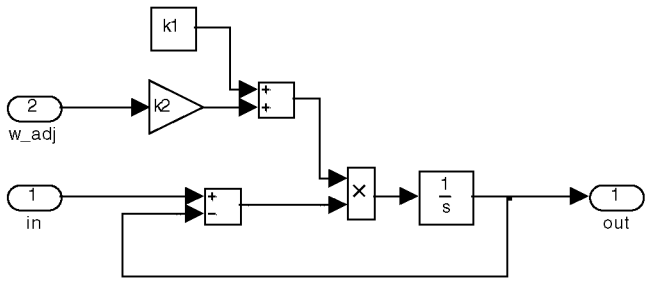

Fig. 8 Adaptive filter for simulation.

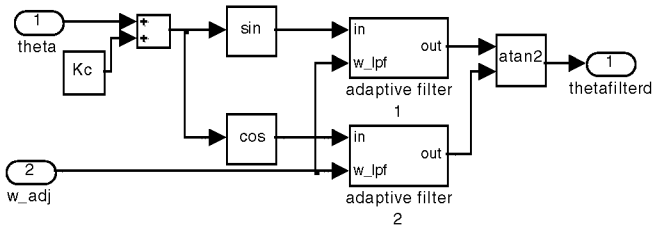

Fig. 9 Adaptive filtering of estimated position.

$$H = \frac{1}{1+\tau s} = \frac{1}{\sqrt{1+(\omega\tau)^2}}e^{-j\theta_f} \tag{33}$$

$$\theta_f = \arctan(\omega\tau) \tag{34}$$

where θ_f is the phase delay of the low pass filter. From (34) it can be seen that the phase delay depends on the frequency. By choosing $\omega\tau$ = constant the phase delay is fixed and hence can be compensated.

During a speed reversal operation, drive instability is a problem as the PMSM may experience 'hunting' at low speeds. As soon as the actual motor speed changes direction, the estimated position based on (30) changes by a factor π according to (32). The estimated speed, however, may not track the speed change simultaneously and hence the position estimation will not be compensated. The motor speed will therefore increase in the original direction and the factor π disappears, whereupon the position estimation is correct again and the drive regains control.

To prevent the above phenonomen from happening, the estimated position is first input to an adaptive filter as shown in Fig. 9. The output from the filter can not change rapidly and this gives the speed estimator time to track the reverse speed and hence to provide the phase angle compensation.

V. Simulation Results

A. Speed Estimation Using Steady-State Equations

Fig. 10 and Fig. 11 shows the MATLAB simulation results of the estimator based on (19) and (22). The real position and speed are applied to the controllers in the control structure as described in Section II. Fig. 10 shows the result of a no-load

drive cycle comprising an acceleration from 0 to 150 rad/s, followed by a deceleration to 100 rad/s and then a further deceleration to 10 rad/s. The gain settings for the PI speed controller are $K_P = 0.2$ and $K_I = 0.1$s.

The results in Fig. 10 and Fig. 11 show that the estimation errors are large during acceleration. At steady state, however, the estimation errors disappear and the position and speed are tracked quite accurately.

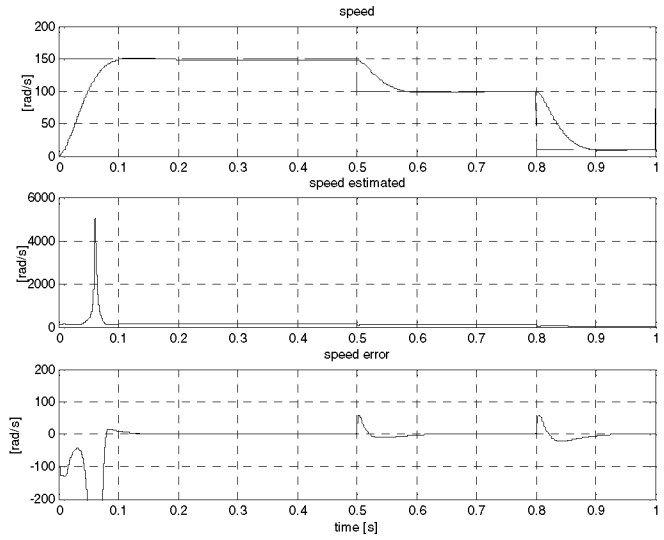

Fig. 10 Speed, estimated speed and speed error: estimation using steady-state equations.

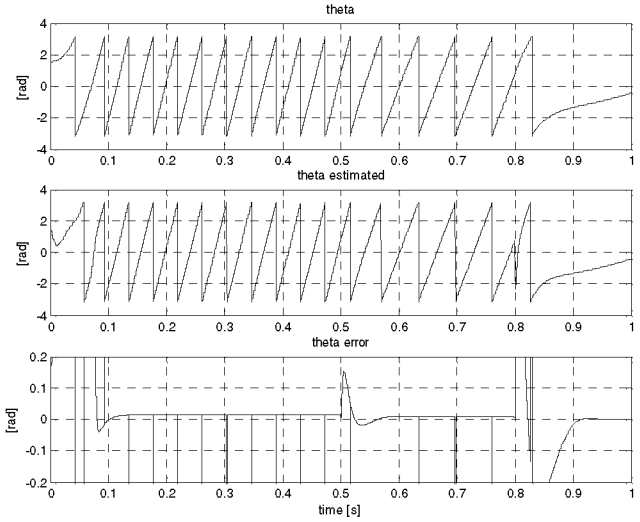

Fig. 11 Position, estimated position and position error: estimation using steady-state equations.

B. *Speed Estimation Using Dynamic Equations*

Fig. 12 and Fig. 13 show simulation results of the estimator based on (30) and (31) implemented in the control structure as described in Section II. For comparison purpose the same drive cycle in Section V-*A* is used.

It is noticed that both the speed and position are well tracked. There is a steady-state error of 0.1% in the speed estimation. Part of the error is attributed to the applied low pass speed filter, which will cause some phase lag at high frequencies.

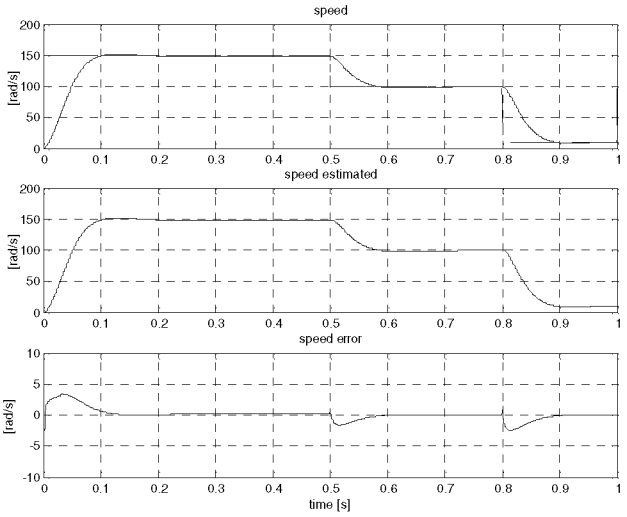

Fig. 12 Speed, estimated speed, speed error: estimation using dynamic equations.

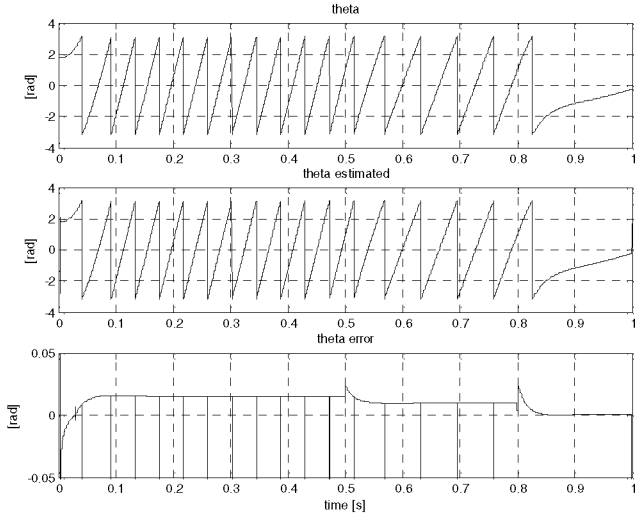

Fig. 13 Position, estimated position and error: estimation using dynamic equations.

C. *Speed Estimation with State Filter and Correction*

Fig. 14 and Fig. 15 show the simulation results using the model illustrated in Fig. 7. The motor drive cycle now comprises an acceleration from 0 to 150 rad/s, then a speed reversal from 150 rad/s to -100 rad/s, and finally a deceleration to -10 rad/s. Again no load is applied for this study.

With this estimation algorithm, the speed error tends to zero at steady-state. The position error at nominal speed is about 0.157 rad. In the zero speed region the speed error becomes larger but the PMSM drive is able to startup from zero speed.

Further simulation results show that the estimator is able to startup and converge from any initial rotor position.

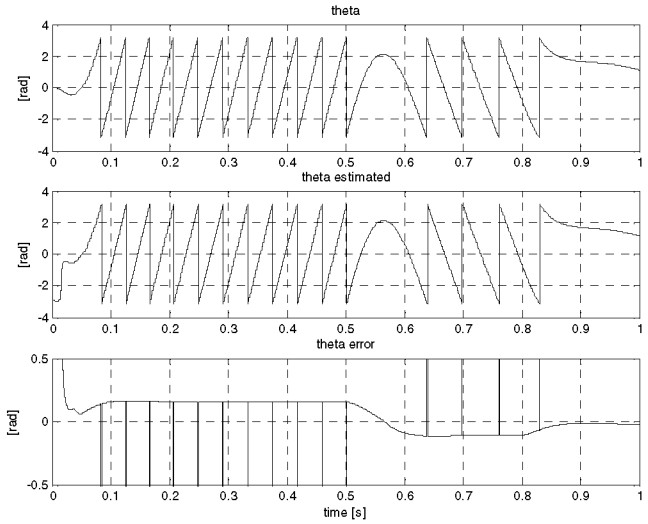

Fig. 14 Position, estimated position and position error, estimation with state filter and correction.

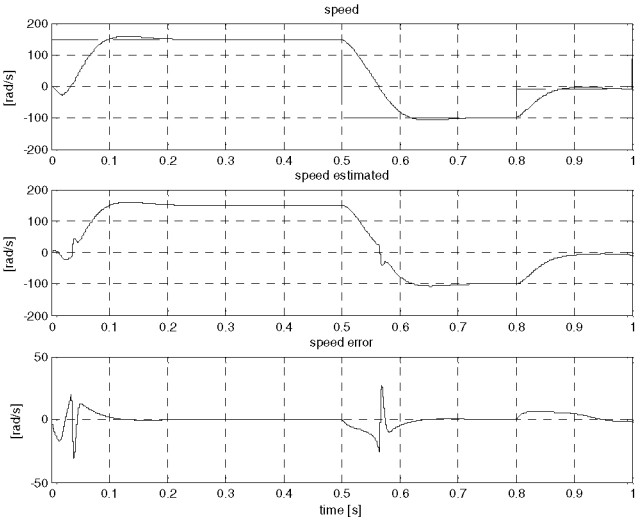

Fig. 15 Speed, estimated speed and speed error, estimation with state filter and correction.

VI. Conclusion

The estimator based on the steady-state equations is shown to have poor performance during transient operation. On the other hand, the estimator based on the dynamic equations with state filter, position correction and adaptive filtering, gives satisfactory performance. Convergence from any initial rotor position and zero speed error during steady-state operation can be achieved. At normal speeds, the estimator also shows good performance under the effect of parameter changes, but the parameters must be accurately known in order to provide a stable startup with small transient errors. The arctangent function employed is sensitive to noise in the estimated back EMF signal. Further research to be undertaken includes the effect of parameter changes during transients and improvement of the drive performance in the presence of noise.

Appendix

Data of PMSM Used in Simulations

Parameter	Symbol	Value
Nominal Power	P_n	600 W
Stator winding self induction	L_s	20.5 mH
Stator winding resistance	R_s	1.55 Ω
Back EMF constant	λ	0.22 V•s/rad
Damping constant	B	2.2 x 10^{-3} N•s/rad
Number of pole-pairs	P	1
Rotor inertia	J	2.2 x 10^{-3} kg•m^2
Nominal speed	ω_n	150 rad/s
Drive current limit	I_{max}	20 A
Drive voltage limit	V_{max}	300V

Acknowledgment

The work described in this paper was fully supported by a grant from the Research Grants Council of the Hong Kong Special Administrative Region (Project No. 5201/03E).

References

[1] P. Pillay and R. Krishnan, "Modeling of permanent magnet motor drives," *IEEE Trans. Industrial Electronics*, vol 35 , no. 4 , Nov. 1988, pp. 537–541.

[2] R. Dhaouadi, N. Mohan and L. Norum, "Design and implementation of an extended Kalman filter for the state estimation of a permanent magnet synchronous motor," *IEEE Trans. Industrial Electronics*, vol. 6 , no. 3 , Jul. 1991, pp. 491–497.

[3] H. Rasmussen, P. Vadstrup, and H. Børsting, "Adaptive sensorless field oriented control of PM motors including zero speed," in *IEEE International Symposium on Industrial Electronics*, May 2004, Ajaccio, France.

[4] K. Rajashekara, A. Kawamura and K. Matsuse, "Sensorless control of AC motor drives", New York: IEEE Press, 1996.

[5] A. R. Munoz, and T. A. Lipo, "On-line dead-time compensation technique for open-loop PWM-VSI drives," *IEEE Trans. Industrial Electronics*, vol. 14, no. 4, Jul. 1999, pp. 683–689.

[6] Hyun-Soo Kim, Hyung-Tae Moon and Myung-Joong Youn, "On-line dead-time compensation method using disturbance observer," *IEEE Trans. Industrial Electronics*, vol. 18, no. 6, Nov. 2003, pp. 1336–1345.

[7] Hyun-Soo Kim, Kyeong-Hwa Kim and Myung-Joong Youn, "On-line dead-time compensation method based on time delay control," *IEEE Trans. Control Systems Technology*, vol. 11, no. 2, Mar. 2003, pp. 279–285.

[8] Atan2 function, http://www.netlib.org.

[9] S. Bolognani, M. Zigliotto and M. Zordan, "Extended-range PMSM sensorless speed drive based on stochastic filtering," *IEEE Trans. Power Electronics*, vol. 16, no. 1, Jan. 2001, pp. 110– 117.